Preprints (www.preprints.org) | NOT PEER-REVIEWED | Posted: 1 April 2021 doi:10.20944/preprints202104.0007.v1

Green Synthesis of Highly Concentrated and Stable Colloidal Dispersion of Core-Shell Silver Nanoparticles (AgNPs-Shell) and their Antimicrobial and Ultra-high Catalytic Properties

Azam Ali [1], Mariyam Sattar [2], Muhammad Humble Khalid Tareen [3], Jiri Militky [1], Fiaz Hussain [3*], Muhammad Tayyab Noman [4]*

mehr_azam91@yahoo.com; fiazravian@gmail.com

[1]*Department of Material and Textile Engineering, Technical University of Liberec, Czech Republic*

[2]*Department of Mechanical Engineering, Institute of Space Technology, Islamabad, Pakistan*

[3]*Institute of advanced materials, Bahauddin Zakariya University, Multan, Pakistan*

[4]*Department of Machinery Construction, CXI, Technical University of Liberec, Czech Republic*

Abstract

The versatile one-pot green synthesis of a highly concentrated and stable colloidal dispersion of AgNPs was carried out using the self-assembled tannic acid without using any other hazardous chemicals. Tannic acid (Plant-based polyphenol) was used as a reducing and stabilizing agent for silver nitrate in a mild alkaline condition. The synthesized AgNPs were characterized for their concentration, capping, size distribution, and shape. The experimental results confirmed the successful synthesis of nearly spherical and highly concentrated (2281 ppm) AgNPs, capped with poly-tannic acid (AgNPs-PTA). The average particle size of AgNPs-PTA was found 9.90 ± 1.60 nm. The colloidal dispersion of synthesized nanoparticles was observed stable for more than 15 months in the ambient environment (25 ^{o}C, 65 % relative humidity). The synthesized AgNPs-PTA showed an effective antimicrobial activity against Staphylococcus Aureus Escherichia coli. Ag-PTA also exhibited enhanced catalytic properties. It reduces 4-nitrophenol into 4-aminophenol in the presence of $NaBH_4$ with a normalized rate constant (K_{nor} = K/m) of 615.04 $mL \cdot s^{-1} \cdot mg^{-1}$. Furthermore, AgNPs-PTA were stable for more than 15 months under ambient conditions. The unique core-shell structure and ease of synthesis render the synthesized nanoparticles superior to others, with potential for large-scale applications, especially in the field of catalysis and biomedical.

KEYWORDS: *Biomedical, Green Synthesis, Silver Nanoparticles, Colloidal stability, Antimicrobial and catalytic activity.*

 doi:10.20944/preprints202104.0007.v1

1 Introduction

Metallic nanoparticles have attracted the attention of scientists and researchers and have found applications in the emerging fields of nanoscience and biomedical technology [1,2]. Among many metallic nanoparticles, silver nanoparticles (AgNPs) are well known for their wide range use for optical, catalytic, electrical, and biomedical applications [3–5]. Generally, AgNPs are prepared by the chemical [6], and physical [7] synthesis methods. The physical and chemical methods for the synthesis of AgNPs involve the use of toxic, costly, and environmentally hazardous materials. Most recently, the green synthesis methods [5] are introduced that allow the use of eco-friendly, cost-effective and nontoxic preparation of AgNPs. Plant-mediated green synthesis of AgNPs has several advantages over the physical and chemical synthesis methods as it is facile, cost-effective, easy to scale up, and eco-friendly [8]. Furthermore, the green synthesis technique results in higher stable dispersions of nanoparticles without using high energy input, high pressure, high temperature, and toxic chemicals [9].

Tannic acid (TA) contains catechol and galloyl groups, which are well known for their metal chelation and material surface binding properties and play a vital role in the green synthesis of nanoparticles at room temperature by acting as both, reducing and capping agent [10,11]. In alkaline conditions, TA polymerizes and forms a capping layer of poly tannic acid [12]. These two properties of TA make it an ideal candidate for the green synthesis of metallic nanoparticles. In the past, several attempts were reported to fabricate tannic acid-mediated nanoparticles and their potential applications in the field of surface-enhanced Raman scattering [13], catalysis [14], treatment of organic pollutants [15], visual detection of ions [16], toxic gas sensing [17], and biomedical [18].

Due to the multi-drug resistant bacteria, it is vital to find alternative means to kill them [19,20]. Ag NPs are well known due to their antimicrobial activity [21]. However, the stability of nanoparticles plays a unique role in their antibacterial activity [22,23]. One method for stabilizing the Ag NPs is to encapsulate them in a shell [24], like Ag NPs-PTA. Additionally, biocompatible TA also exhibits antibacterial activity [25]. Ag NPs are also reported to exhibit good catalytic properties for the reduction of environmental pollutants. It has been found that higher stability and better dispersion of nanocatalysts, due to the shell, results in enhanced catalytic activity. Therefore, the unique self-polymerization and reducing properties of TA were utilized for the facile synthesis of highly concentrated and stable dispersion of Ag NPs-PTA.

Ag NPs-PTA were characterized for their concentration, capping, size distribution, shape, stability, antibacterial, and catalytic properties. The experimental results show the successful synthesis of nearly spherical and highly concentrated (2281 ppm) Ag NPs, capped with poly-tannic acid (Ag NPs-PTA). The average particle size of Ag NPs-PTA was found 9.90 ± 1.60 nm. The colloidal dispersion of synthesized nanoparticles was observed stable for more than 15 months in the ambient environment. To the best of the authors' knowledge, it is the first time that such an effective antimicrobial agent and reduction catalyst with high concentration and high colloidal stability are prepared by green synthesis method.

Preprints (www.preprints.org) | NOT PEER-REVIEWED | Posted: 1 April 2021 doi:10.20944/preprints202104.0007.v1

2 Experimental Work

2.1 Materials

Silver nitrate ($AgNO_3$), tannic acid ($C_{76}H_{52}O_{46}$, 1701.01 g/mol), sodium borohydride ($NaBH_4$), 4-nitrophenol (4-NP), and sodium hydroxide (NaOH) were supplied by Sigma-Aldrich. Ultrapure deionized (DI) water, collected from a Milli-Q SP reagent water system (Millipore, Milford, MA), was used during the synthesis process. All the chemicals were used as received without any purification. Luria-Bertani (LB) broth with agar (Lennox) and LB broth (Lennox) was supplied by Merck for anti-bacterial analysis. Freshly prepared solutions of all the chemicals were used during all chemical reactions.

2.2 Synthesis of Ag NPs-PTA

The synthesis of Ag NPs-PTA was carried out by one-pot mixing of 10 ml $AgNO_3$ (0.147 M), 35 ml TA (1 mM) and 1.35 ml of NaOH (0.2 M) in the ambient environment. The suspension was vigorously mixed using a magnetic stirrer for 10 minutes to produce a homogenous mixture followed by heating at 45 ºC for 30 minutes stirring at 250 RPM. The solution was cooled down to room temperature and the freshly prepared nanoparticles were collected by centrifugal separation (1100 RPM for 15 minutes) and were washed three times using DI water. Figure 1 shows a schematic of the steps involved in this novel method of Ag NPs preparation.

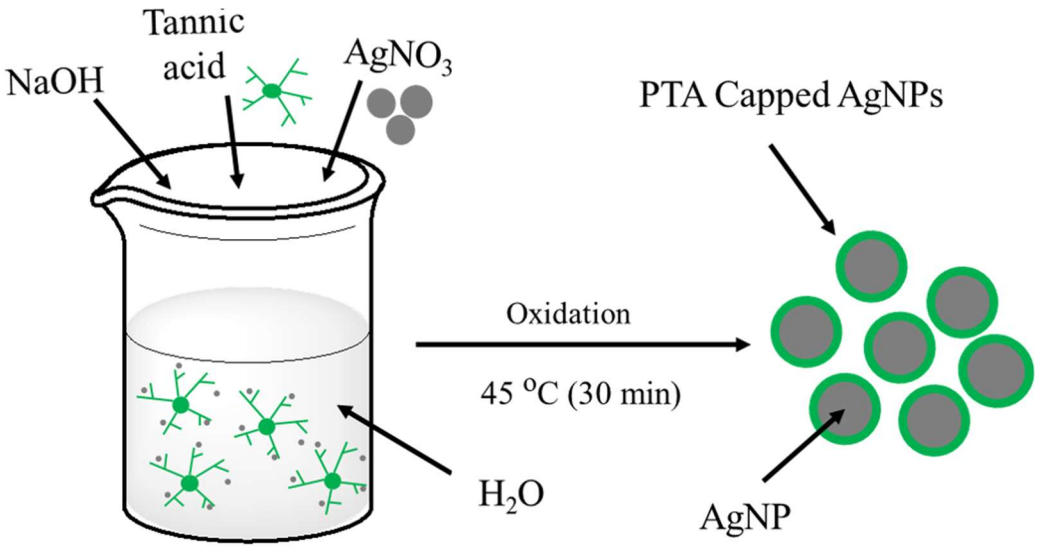

Figure 1. The schematic diagram for the green synthesis of Ag NPs-PTA**.**

Ag NPs-PTA dispersion was applied to the Activated Carbon Fibre (ACF) sheets (round shape and 1.5 cm in diameter) by drop-coating method followed drying in the vacuum oven at 50 ºC for 2 hours. Four ACF sheets were placed in the tissue culture plate. The aqueous solution of nanoparticles was drop coated in a way to obtain 0.5 mg, 1 mg, 2 mg,

Preprints (www.preprints.org) | NOT PEER-REVIEWED | Posted: 1 April 2021 doi:10.20944/preprints202104.0007.v1

and 4 mg final concentration of nanoparticles on the samples, respectively. The samples coated with nanoparticles were placed overnight in the vacuum oven for drying at 50 ºC.

2.3 Characterization

The successful synthesis of Ag NPs-PTA was confirmed by measuring the ultraviolet-visible (UV-Vis) spectrum using a spectrophotometer (Model: JASCO V-770). The absorption spectrum of the nanoparticle's dispersion was analyzed in the range of 200 to 700 nm. The size distribution, shape, surface morphology, and other physical properties of the particles were examined by using Schottky Field Emission Scanning Electron Microscopy (FE-SEM, Model: JEOL JSM-7600F) at an accelerating voltage of 15 kV and High-Resolution Transmission Electron Microscopy (HR-TEM, Model: JEM-3010). Samples were prepared by drop coating of aqueous solution on the carbon-coated copper grid for morphological analysis of Ag NPs-PTA by TEM. Elemental analysis of the Ag NPs-PTA was evaluated with the help of an energy dispersive spectrometer (EDS, Model: X-MAX 50).

Zeta-potential analysis of the sample was conducted in water with the help of Zeta sizer Malvern Instruments (Model: Nano-SZ). Inductively Coupled Plasma Mass Spectroscopy (ICP-MS, Model: Agilent 7500) was used to determine the actual concentration of the product. The chemical composition of Ag NPs-PTA was also confirmed by an X-Ray Photoelectron Spectrometer (XPS, Model: ESCALAB250).

2.4 Antimicrobial Tests

The Antimicrobial activity of synthesized nanoparticles was analyzed against Gram-negative, Escherichia coli (E. coli, ATCC1129) and Gram-positive, Staphylococcus aureus (S. aureus, ATCC 6538). The AATC147-2004 standard zone of inhibition test was adopted to determine the Antimicrobial performance of synthesized Ag NPs-PTA [26]. The Luria-Bertani (LB) agar solution (25 ml) was added to the agar plates and were placed into a refrigerator for 15 minutes. 50 µl of fresh suspension of bacterial strains (E. coli and S. aureus, 10^5 -10^6 CFU per ml) was transferred to LB agar plates. Bacterial colonies were spread gently in the plate surface with the help of a sterilized glass rod. Round shape ACF samples (1.5×1.5 cm) containing 0.5 mg, 1 mg, 2 mg, and 4 mg concentrations of synthesized Ag NPs-PTA were placed in the LB agar plates along with the reference (control) ACF sample (without Ag NPs-PTA). LB agar plates having ACF samples were placed into the incubator at 37 ºC for 24 hours. The zones of inhibition around the samples were measured to determine the antimicrobial activity of Ag NPs-PTA.

2.5 Catalytic reduction of 4-NP

The catalytic reduction of the 4-NP into 4-AP in the presence of excess $NaBH_4$ was carried out to analyze the catalytic activity Ag NPs-PTA. Briefly, 2 mL of fresh DI water, 1 mL of freshly prepared $NaBH_4$ (1 M), and 100 µL 4-NP (5 mM) were added into a cuvette with constant mechanical stirring. To determine the catalytic reduction of the 4-NP, 50 µL of the prepared nanocatalysts (1 mM) was added to the mixture. To monitor the reaction progress, the UV-visible spectrum of the solution was measured at different intervals of time.

Preprints (www.preprints.org) | NOT PEER-REVIEWED | Posted: 1 April 2021 doi:10.20944/preprints202104.0007.v1

3 Results and Discussion

UV-Vis absorption spectrophotometer was used to confirm the successful synthesis of Ag NPs-PTA. Figure 2 represents the characteristic UV-Vis spectrum of the synthesized Ag NPs-PTA nanoparticle dispersion. The concentrated sample was diluted 300 times for UV-Vis analysis. The results, figure 2, shows a sharp absorption at 440 nm, which is a typical surface plasmon resonance absorbance band for Ag NPs-PTA [12].

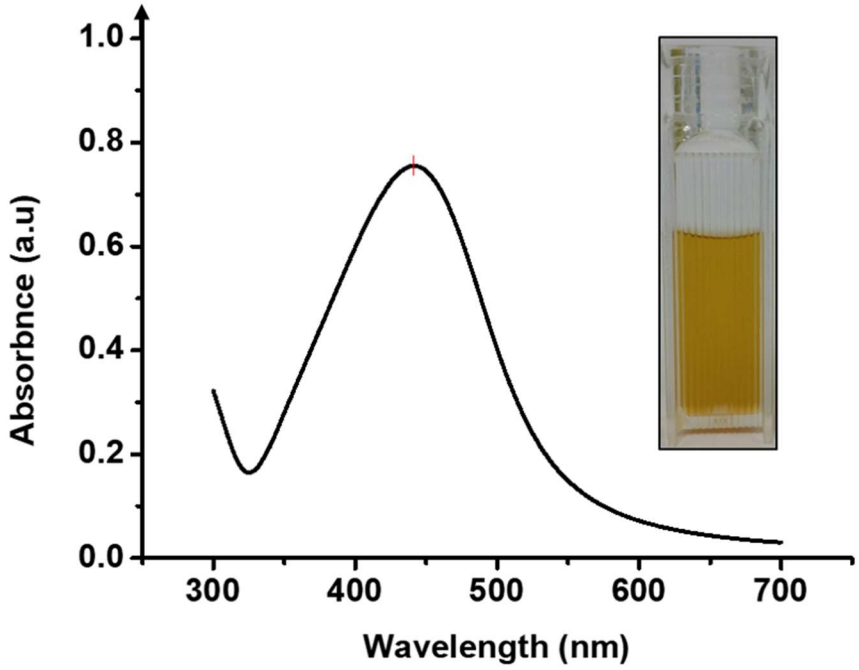

Figure 2. UV-Vis spectrum of the nanoparticle dispersion.

Figures 3(a) and 3(b) represent the FE-SEM and HR-TEM analysis results for the surface morphology of the synthesized Ag NPs-PTA. Spherical-shaped nanoparticles with an average particle size of ~ 9.90 ± 1.60 nm (determined by using ImageJ software) were observed and the corresponding size distribution histogram is shown in figure 3(c). The EDS results, figure 3(d), shows the presence of Ag, C, and O elements and thus confirm the synthesis of pure Ag NPs-PTA nanocomposites. A prominent peak, (figure 3d) was observed at 3 keV due to the characteristic surface plasmon resonance of the silver nanocomposites while the shorter peaks are attributed to the capping agent of the particles and silicon wafer substrate. A similar observation is reported by other researchers while analyzing the EDS results for silver nanoparticles [27].

Preprints (www.preprints.org) | NOT PEER-REVIEWED | Posted: 1 April 2021 doi:10.20944/preprints202104.0007.v1

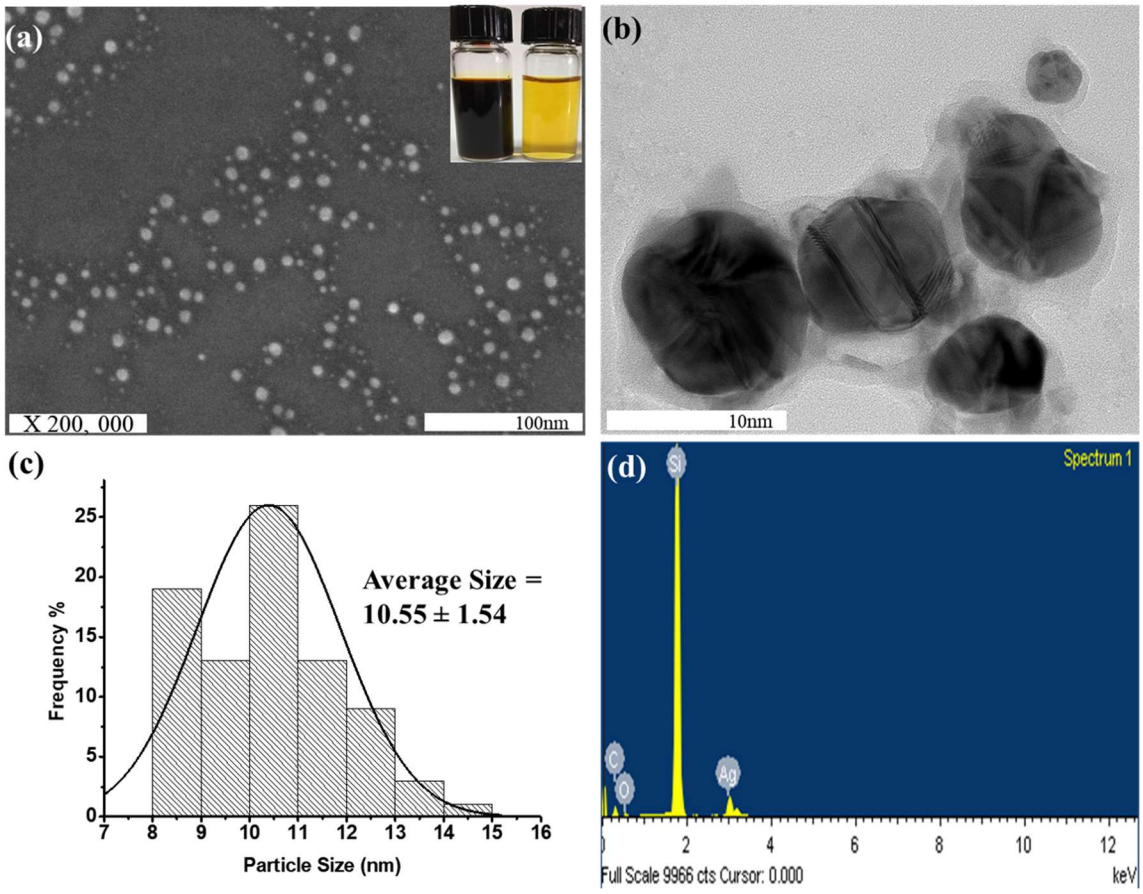

Figure 3. (a) SEM image of nearly monodispersed Ag NPs-PTA, (inset is the optical images of concentrated (left) and diluted (right) colloidal dispersion of Ag NPs-PTA); (b) HR-TEM image of nanoparticles; (c) Size distribution analysis of Ag NPs-PTA; and (d) EDS pattern of synthesized Ag NPs-PTA.

The Zeta potential value, to analyze the electrostatic stability of the Ag NPs-PTA, was found to be -18.8 ± 1.48 mV, which indicates the high aqueous stability of these nanoparticles. The actual concentration of obtained Ag NPs-PTA, determined by ICP-MS, was found 2281 ppm. To the best of our knowledge, it is the first time that such a high concentration of Ag NPs has been successfully synthesized by a green synthesis process. Characteristics of synthesized nanoparticles are summarized in table 1 and compared with the previously reported data for comparison purposes.

The chemical composition of Ag NPs-PTA was analyzed by the XPS and corresponding results are shown in figure 4 (a & b). Fei et al. analyzed the tannic acid under XPS and reported C and O as the main components of the tannic acid [12]. The XPS results, reveals that AgNPs-PTA sample contains a very small quantity of silver as compared to other elements and confirms the Ag as a core and PTA as a capping layer and hence confirms the synthesis of core-shell (Ag NPs-PTA) nanoparticles. Moreover, the binding energy peaks of C 1s shift from 284.79 to 285.41 and O 1s shifts from 532.23 to 532.79 in Ag NPs-PTA compared to pure TA due to the oxidation of tannic acid [12].

Preprints (www.preprints.org) | NOT PEER-REVIEWED | Posted: 1 April 2021 doi:10.20944/preprints202104.0007.v1

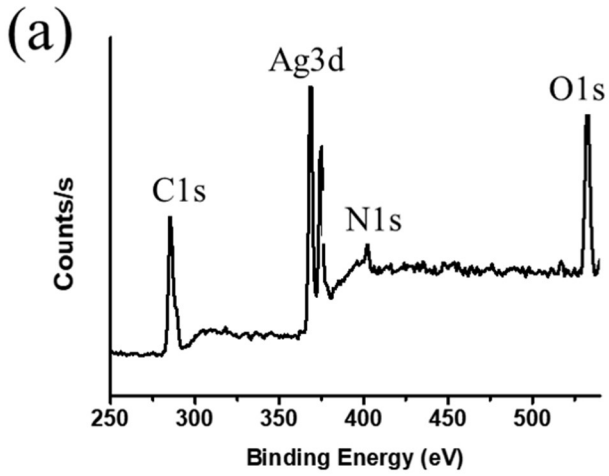

(b)

Element	Peak BE	Atomic %
Ag3d	368.37	5.85
O1s	532.79	26.79
C1s	285.41	55.7

Figure 4. (a) X-ray photoelectron (XPS) analysis of Ag NPs-PTA; (b) elemental composition of synthesized silver nanoparticles.

To analyze the long-term stability of the Ag NPs-PTA, the sample was aged for 15 months in ambient conditions. Figure 5 (a) shows the UV-Vis spectra of the freshly prepared Ag NPs-PTA solution and Ag NPs-PTA solution aged for 15 months. The UV-Vis spectrum of the aged Ag NPs-PTA is almost similar to the UV-Vis spectrum of the fresh Ag NPs-PTA indicating that nanoparticles did not aggregate even after 15 months of shelf life. The Zeta potential values and the color of the Ag NPs-PTA dispersion before and after aging were also observed unchanged, figure 5 (b). The analyzed results, Zeta potential, color, and UV-Vis spectra, of the fresh and aged Ag NPs-PTA, confirm their long-term stability. TEM analysis also confirmed that nanoparticles do not aggregate even after 15 months of shelf life (data not shown).

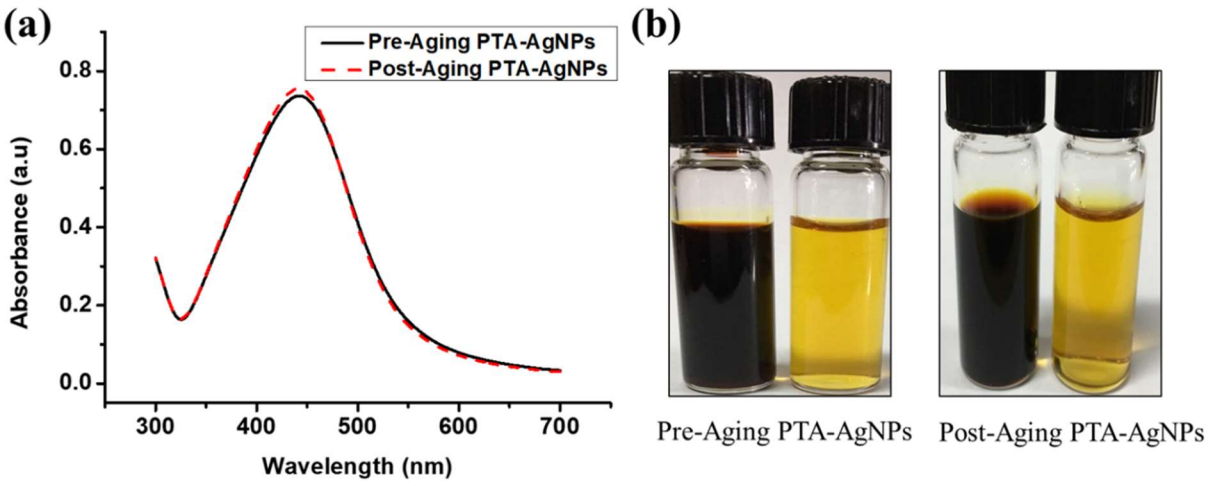

Figure 5. (a) UV-Vis spectra of freshly prepared Ag NPs-PTA solution and Ag NPs-PTA solution after 15 months of storage in a dark ambient environment; (b) Concentrated and diluted samples of synthesized Ag NPs-PTA before and after aging of 15 months.

Preprints (www.preprints.org) | NOT PEER-REVIEWED | Posted: 1 April 2021 doi:10.20944/preprints202104.0007.v1

Table 1. Characteristics of synthesized Ag NPs synthesized in this study in comparison with those synthesized previous studies

Initial $AgNO_3$ Concentration. (M)	*Synthesis time/Aqueous stability*	*Limitation of the synthesis process*	*Particle size (nm)*	*Synthesis method*	*Ref.*
0.147	30 mint/ >15 months	Relatively lower conversion	9	Green chemistry	Current Study
1.9	25 h/-	Long reaction time under extreme precautions	30	Chemical	[28]
1.65	2 h/3 months	Long reaction time, no reproducibility, broad size distribution	20-230	Chemical	[29]
0.94	0.75 h/ 6 months	A relatively high temperature is required. Particles are not stable at low/mild alkaline condition	5-80	Chemical	[30]
0.83	0.75 h/14 months	Use of toxic chemicals	14	Chemical	[4]
0.43	10 h/-	High energy input (200 W), long reaction time, and use of environmentally hazardous materials	20-30	Microwave	[31]
0.27	7 min/-	Not stable at higher concentrations (>0.3M)	26	Chemical	[32]
0.16	4.5 h/-	Two-phase, complicated process	4	Chemical	[33]
0.02	2 mint/-	Relatively low concentration and use of hazardous and toxic chemicals	10	Chemical	[34]

Preprints (www.preprints.org) | NOT PEER-REVIEWED | Posted: 1 April 2021 doi:10.20944/preprints202104.0007.v1

3.1 Antimicrobial Response Analysis

The ACF sheets were drop coated with Ag NPs-PTA dispersion to analyze the antimicrobial response of the synthesized Ag NPs-PTA. In general, nanoparticles easily release from the ACF sheet and they can effectively kill the microbes [35]. Figure 6 represents the SEM images of the ACF sheets drop coated with (b & c) and without (a) AgNPs-PTA dispersion. The results, in figure 6, show that the Ag NPs-PTA are not aggregated and are homogeneously distributed on the ACF sheet surface which is beneficial for antimicrobial applications.

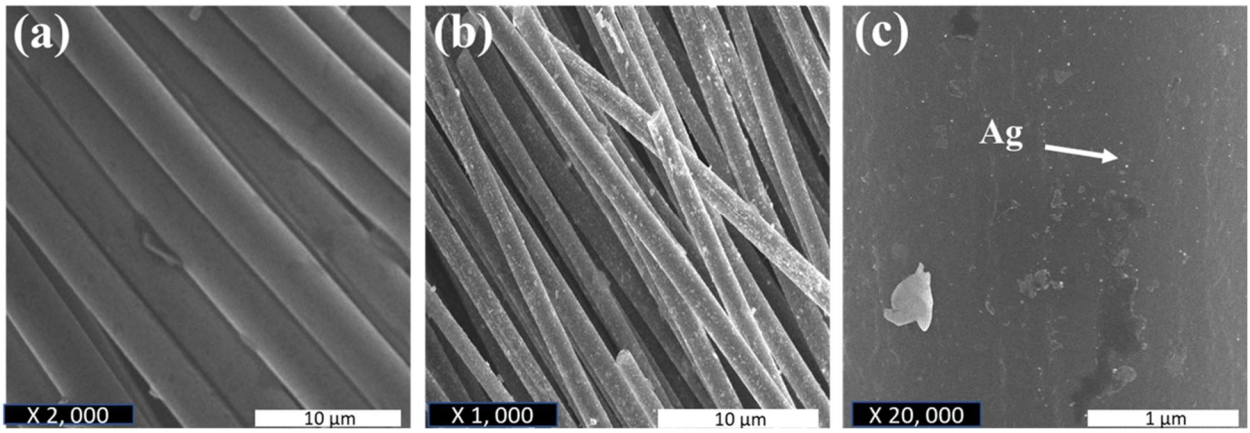

Figure 6. (a) Surface morphology of ACF sheet; (b) Surface morphology of ACF sheet loaded with synthesized Ag NPs; (c) corresponding magnified image of ACF containing dispersed Ag NPs-PTA.

The antimicrobial response of the Ag NPs-PTA was analyzed using the standard Zone of Inhibition test. For this, antimicrobial activity of ACF sheets drop coated with and without Ag NPs-PTA, having different concentration of Ag NPs-PTA (0.0 (Reference/Control), 0.5 mg, 1.0 mg, 2.0 mg, 4.0 mg, respectively) was analysed against S. aureus, figure 7 (a) and E. coli , figure 7 (b), microbes. It was observed that the reference/control sample (C) show no inhibition against the antimicrobe while the ACF sheets drop coated with Ag NPs-PTA dispersion displayed remarkable antimicrobial performance and a clear Zone of Inhibition (ZOI) was noticed. Furthermore, this antimicrobial response lasted for around 8 days. The values of ZOI for each sample are reported in table 2. The results indicate that the Ag NPs-PTA dispersion is more effective towards E. coli compared to S. aureus. This could be due to the thin (7-8 nm) peptidoglycan layer (protecting layer) of E. coli compared to S. aureus (20-80 nm). Several other researchers also reported similar observations [36,37].

Preprints (www.preprints.org) | NOT PEER-REVIEWED | Posted: 1 April 2021 doi:10.20944/preprints202104.0007.v1

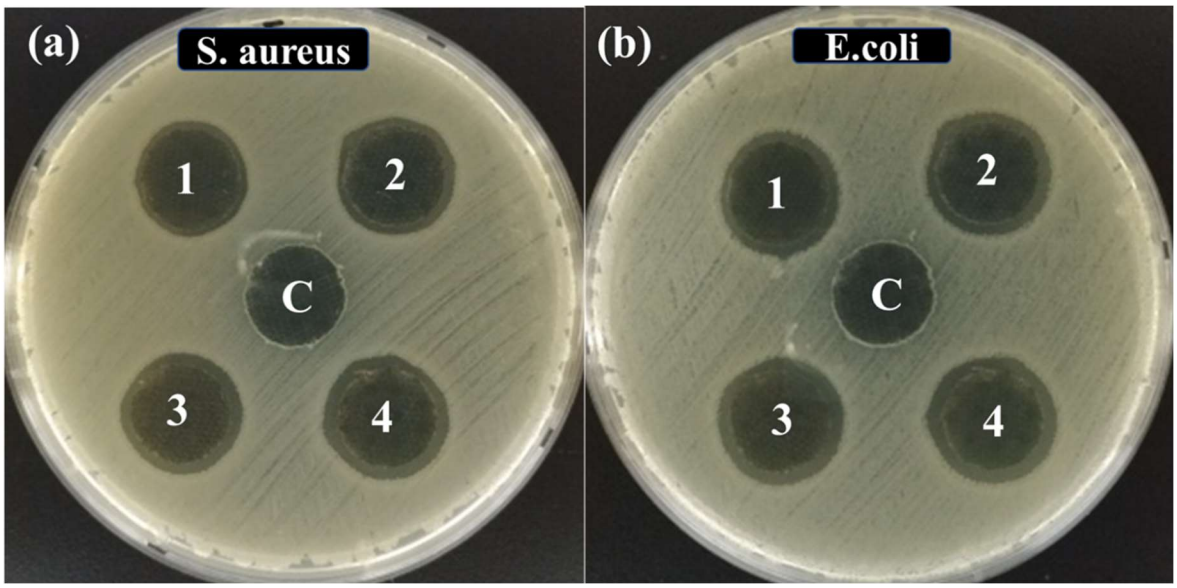

Figure 7. Zone of Inhibition (ZOI) of samples (1, 2, 3, 4, and C, containing different concentrations of Ag NPs-PTA) measured against (a) S. aureus and (b) E. coli microbial stains.

Table 2. Antimicrobial activity (ZOI) of the ACF sheet, containing different amount of Ag NPs measured against S. aureus and E. coli.

Sample	*Amount of silver (mg)*	*Zone of inhibition against E. coli (mm)*	*Zone of inhibition against S. aureus (mm)*
Control (C)	0	0	0
1	0.5	1.5	0.7
2	1	1.5	1.5
3	2	2	1.5
4	4	2	2.0

3.2 Catalytic Reduction of 4-NP

In addition to antimicrobial properties, synthesized Ag NPs-PTA nanocomposites also exhibited enhanced catalytic properties. The reduction of 4-NP to 4-AP was analyzed in the presence of excess $NaBH_4$. This model reduction reaction was monitored by UV-Vis spectroscopy at different intervals of time. As shown in Fig. 8, after the addition of Ag NPs-PTA nanocomposites, the characteristic absorption peak of 4-NP at 400 nm continues to decrease with time, while a new peak at 300 nm, attributed to 4-aminophenol (4-AP), increases slowly and simultaneously. The characteristic yellow color of the 4-NP disappeared completely after the completion of the reaction. It is important to note that, in the absence of synthesized nanocatalyst, characteristics yellow color and absorption peak of 4-NP (λ =400 nm) does not change even after 24 hours of incubation.

Preprints (www.preprints.org) | NOT PEER-REVIEWED | Posted: 1 April 2021 doi:10.20944/preprints202104.0007.v1

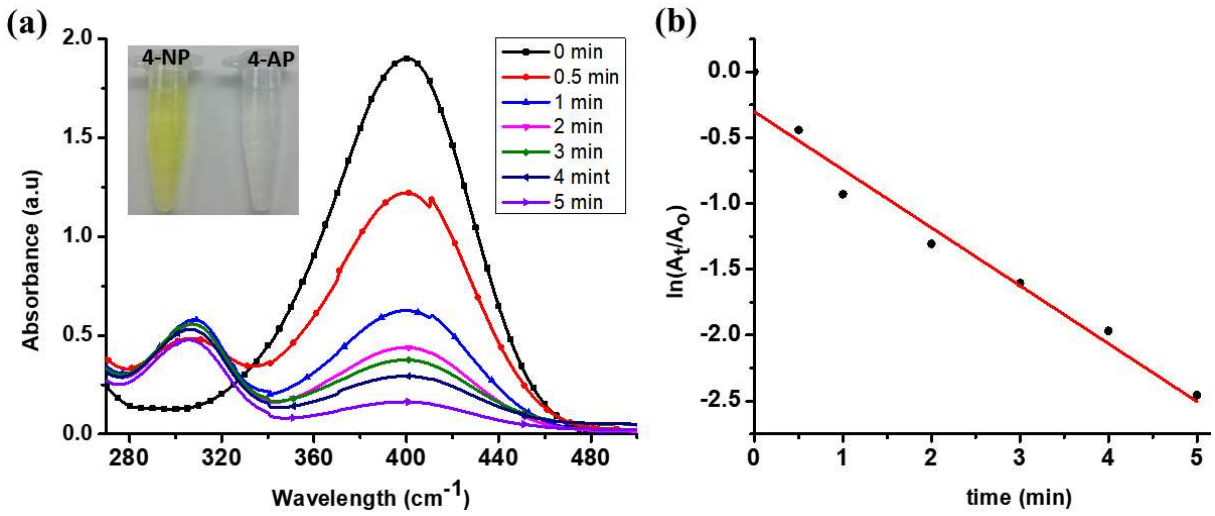

Figure 8. (a) UV-Vis spectra of the catalytic conversion of 4-NP to 4-AP in the presence of Ag NPs-PTA; (b) Plot of $\ln(A_t/A_o)$ versus time for the reduction of 4-NP into 4-AP in the presence of Ag NPs-PTA nanocatalyst.

The catalytic reaction follows pseudo-first-order kinetics in the presence of excess $NaBH_4$. For the normalization of C_t to C_0, A_t was divided by A_0 at 400 nm (where C_0 is the initial concertation and C_t is the concentration of 4-NP at certain time t. Similarly, A_0 is the initial absorption and A_t is the absorption of 4-NP at certain time t). The rate constant (from slope of dependence $\ln(A_t/A_0)$ on time t obtained by least squares) for this reaction was 8.18×10^{-2}. A normalized rate constant K_{nor} = K/m (where m is the amount of silver [mg/mL] loaded for catalytic activity) was calculated to nullify the effect of the metal loading concentration. It is evident from the results (K_{nor}) summarized in Table 3 that the catalytic activity of synthesized Ag NPs-PTA nanocatalyst for the reduction of organic pollutant 4-NP was superior when compared to previously reported silver-based catalysts.

To the best of our knowledge, this is one of the highest rate constants reported for the reduction of 4-NP. This enhanced catalytic performance can be attributed to the synergistic effect of the silver nanoparticles, PTA shells, and the smaller Ag NPs-PTA nanocomposites compared to the previously reported data. The PTA shell of the nanocatalysts has abundant aromatic rings, which interact and improve the localized concentration of 4-NP and BH^{-4} from the aqueous solution through π-π stacking interactions and thus contribute to the enhanced catalytic efficiency of the nanoparticles in the 4-NP reduction.

Preprints (www.preprints.org) | NOT PEER-REVIEWED | Posted: 1 April 2021 doi:10.20944/preprints202104.0007.v1

Table 3. Catalytic activities of Ag NPs-PTA nanocomposites for the 4-NP reduction in comparison with previously reported silver-based nanocatalysts

Nanocatalyst structure	Catalyst (mg/mL)	Rate constant K (s^{-1})	$K_{nor.}$ ($mL \cdot s^{-1} \cdot mg^{-1}$)	Reference
Halloysite nanotubes-Ag	8.00×10^{-3}	6.96×10^{-7}	8.70×10^{-5}	[38]
Ag@PAA	2.97×10^{-2}	15.45×10^{-3}	4.59×10^{-4}	[39]
Ag-NP/C composite	1.00×10^{-0}	1.69×10^{-3}	1.69×10^{-3}	[40]
EPS–Ag nanocomposites	2.60×10^{-2}	1.26×10^{-3}	4.80×10^{-2}	[41]
Ag NPs@PAA	2.03×10^{-4}	7.6×10^{-2}	374.94	[4]
TSC-Ag-1.4	1.33×10^{-3}	3.64×10^{-4}	2.7×10^{-1}	[42]
Fe_3O_4/SiO_2-Ag	2.00×10^{-2}	5.50×10^{-3}	2.8×10^{-1}	[43]
Fe_3O_4-@C@Ag	1.00×10^{-2}	3.72×10^{-3}	3.7×10^{-1}	[44]
TAC-Ag-1.4	1.33×10^{-3}	1.65×10^{-3}	1.24	[42]
Fe_3O_4-@C@Ag-Au	1.00×10^{-2}	15.80×10^{-3}	1.58	[44]
AgNP-PG-5K	4.00×10^{-3}	5.50×10^{-3}	1.38	[45]
Ag/SiO_2 1.08	1.1×10^{-3}	2.53×10^{-3}	2.30	[46]
Graphene oxide/Ag NPs−Fe_3O_4	8.1×10^{-3}	2.67×10^{-2}	3.30	[47]
TAC-Ag-1.0	1.33×10^{-3}	5.19×10^{-3}	3.90	[42]
Ag NPs@PGMA-SH composite	9.00×10^{-4}	3.94×10^{-3}	4.38	[48]
AgNPs-PTA	1.33×10^{-4}	8.18×10^{-2}	615.04	Our work

4 Conclusion

In this research work, highly concentrated and stable colloidal dispersion of Ag NPs-PTA was synthesized using a novel, one-pot, and cost-effective green synthesis method. Nontoxic tannic acid was used for the fabrication of Ag NPs, as a strong reducing and capping agent under mild alkaline conditions. The synthesized nanoparticles displayed excellent colloidal stability in the ambient environment (more than 15 months). The synthesized Ag NPs-PTA were characterized, which confirmed the formation of nearly spherical shaped Ag NPs, with the average particle size of ~9.90 ± 1.60 nm and capped with PTA. The Zeta Potential and UV-Vis analysis showed electrostatic and compositional stability of the synthesized Ag NPs-PTA dispersion before and after 15 months aging. The ACF sheet

 doi:10.20944/preprints202104.0007.v1

samples drop coated with Ag NPs-PTA displayed remarkable Antimicrobial response when analyzed against S. aureus, and E. coli microbes. The synthesized Ag NPs-PTA nanocatalyst also displayed an enhanced catalytic performance for the reduction 4-NP to 4-AP with rate constant of (K_{nor}) 63.71 $mL \cdot s^{-1} \cdot mg^{-1}$. This study may offer a unique opportunity for the fabrication of multifunctional metal-PTA nanocomposites, which will have many unique futures uses like catalytic, metal detection, and biomedical applications.

5 Acknowledgment

This work was supported by the Ministry of Education, Youth and Sports of the Czech Republic and the European Union - European Structural and Investment Funds in the frames of Operational Programme Research, Development and Education - project Hybrid Materials for Hierarchical Structures (HyHi, Reg. No. CZ.02.1.01/0.0/0.0/16_019/0000843).

References

1. Agnihotri S, Mukherji S, Mukherji S (2014) Size-controlled silver nanoparticles synthesized over the range 5-100 nm using the same protocol and their antibacterial efficacy. RSC Adv 4:3974–3983. https://doi.org/10.1039/c3ra44507k
2. A. Ali, V. Baheti, J. Militky, Z. Khan, V. Tunakova and S. Naeem, Copper coated multifunctional cotton fabrics, J. Ind. Text. 48 (2017) 448–464
3. An Q, Yu M, Zhang Y, et al (2012) Fe 3O 4@carbon microsphere supported Ag-Au bimetallic nanocrystals with the enhanced catalytic activity and selectivity for the reduction of nitroaromatic compounds. J Phys Chem C 116:22432–22440. https://doi.org/10.1021/jp307629m
4. Andjelković M, Van Camp J, De Meulenaer B, et al (2006) Iron-chelation properties of phenolic acids bearing catechol and galloyl groups. Food Chem 98:23–31. https://doi.org/10.1016/j.foodchem.2005.05.044
5. Baruah B, Gabriel GJ, Akbashev MJ, Booher ME (2013) Facile synthesis of silver nanoparticles stabilized by cationic polynorbornenes and their catalytic activity in 4-nitrophenol reduction. Langmuir 29:4225–4234. https://doi.org/10.1021/la305068p
6. Cao Y, Zheng R, Ji X, et al (2014) Syntheses and characterization of nearly monodispersed, size-tunable silver nanoparticles over a wide size range of 7-200 nm by tannic acid reduction. Langmuir 30:3876–3882. https://doi.org/10.1021/la500117b
7. Cho KH, Park JE, Osaka T, Park SG (2005) The study of antimicrobial activity and preservative effects of nanosilver ingredient. Electrochim Acta 51:956–960. https://doi.org/10.1016/j.electacta.2005.04.071
8. Dong G, Liu H, Yu X, et al (2018) Antimicrobial and anti-biofilm activity of tannic acid against Staphylococcus aureus. Nat Prod Res 32:2225–2228. https://doi.org/10.1080/14786419.2017.1366485
9. Fang Y, Tan J, Choi H, et al (2018) Highly sensitive naked eye detection of Iron (III) and H_2O_2 using poly-(tannic acid) (PTA) coated Au nanocomposite. Sensors Actuators, B Chem 259:155–161.

https://doi.org/10.1016/j.snb.2017.12.031

10. Faupel F, Zaporojtchenko V, Strunskus T, Elbahri M (2010) Metal-polymer nanocomposites for functional applications. Adv Eng Mater 12:1177–1190. https://doi.org/10.1002/adem.201000231
11. A. Ali, V. Baheti, J. Militky, Z. Khan, Utility of silver-coated fabrics as electrodes in electrotherapy applications, J. Appl. Polym. Sci. 135 (2018) 46357. doi:10.1002/app.46357.
12. Ghaffari-Moghaddam M, Hadi-Dabanlou R (2014) Plant mediated green synthesis and antibacterial activity of silver nanoparticles using Crataegus douglasii fruit extract. J Ind Eng Chem 20:739–744. https://doi.org/10.1016/j.jiec.2013.09.005
13. Horecha M, Kaul E, Horechyy A, Stamm M (2014) Polymer microcapsules loaded with Ag nanocatalyst as active microreactors. J Mater Chem A 2:7431. https://doi.org/10.1039/c4ta00606b
14. Huang Q, Shen W, Xu Q, et al (2014) Properties of polyacrylic acid-coated silver nanoparticle ink for inkjet printing conductive tracks on paper with high conductivity. Mater Chem Phys 147:550–556. https://doi.org/10.1016/j.matchemphys.2014.05.030
15. Hussain F, Khurshid MF, Masood R, Ibrahim W (2017) Developing antimicrobial calcium alginate fibres from neem and papaya leaves extract. J Wound Care 26:778–783. https://doi.org/10.12968/jowc.2017.26.12.778
16. Hussain F, Shaban SM, Kim J, Kim D-H (2019) One-pot synthesis of highly stable and concentrated silver nanoparticles with enhanced catalytic activity. Korean J Chem Eng 36:988–995. https://doi.org/10.1007/s11814-019-0270-6
17. Jin R (2015) Atomically precise metal nanoclusters: stable sizes and optical properties. Nanoscale 7:1549–1565. https://doi.org/10.1039/C4NR05794E
18. Jin R, Zeng C, Zhou M, Chen Y (2016) Atomically precise colloidal metal nanoclusters and nanoparticles: fundamentals and opportunities. Chem Rev 116:10346–10413. https://doi.org/10.1021/acs.chemrev.5b00703
19. Kästner C, Thünemann AF (2016) Catalytic reduction of 4-Nitrophenol using silver nanoparticles with adjustable activity. Langmuir 32:7383–7391. https://doi.org/10.1021/acs.langmuir.6b01477
20. Kheybari S, Samadi N, Hosseini S V, et al (2010) Synthesis and antimicrobial effects of silver nanoparticles produced by chemical reduction method. J Pharm Sci 18:168–172
21. A. Ali, V. Baheti, Militky J, Vik. M, “Copper electroless plating of cotton fabrics after surface activation with deposition of silver and copper nanoparticles” Journal of Physics and chemistry A. vol. 137, 2020
22. Lee D, Lee SJ, Moon JH, et al (2018) Preparation of antibacterial chitosan membranes containing silver nanoparticles for dental barrier membrane applications. J Ind Eng Chem 66:196–202. https://doi.org/10.1016/j.jiec.2018.05.030
23. Lee H, Ryu D, Choi S, Lee D (2011) Antibacterial activity of silver-nanoparticles against Staphylococcus aureus and Escherichia coli. Korean J Microbiol Biotechnol 39:77–85. https://doi.org/10.5897/AJMR2016.7908
24. Liu P, Zhao M (2009) Silver nanoparticle supported on halloysite nanotubes catalyzed reduction of 4-nitrophenol (4-NP). Appl Surf Sci 255:3989–3993. https://doi.org/10.1016/j.apsusc.2008.10.094

25. Magdassi S, Grouchko M, Berezin O, Kamyshny A (2010) Triggering the sintering of silver nanoparticles at room temperature. ACS Nano 4:1943–1948. https://doi.org/10.1021/nn901868t
26. Park HJ, Park S, Roh J, et al (2013) Biofilm-inactivating activity of silver nanoparticles: A comparison with silver ions. J Ind Eng Chem 19:614–619. https://doi.org/10.1016/j.jiec.2012.09.013
27. Qasim M, Udomluck N, Chang J, et al (2018) Antimicrobial activity of silver nanoparticles encapsulated in poly-N-isopropylacrylamide-based polymeric nanoparticles. Int J Nanomedicine 13:235–249. https://doi.org/10.2147/IJN.S153485
28. Qu JC, Ren CL, Dong YL, et al (2012) Facile synthesis of multifunctional graphene oxide/AgNPs-Fe3O4 nanocomposite: A highly integrated catalysts. Chem Eng J 211–212:412–420. https://doi.org/10.1016/j.cej.2012.09.096
29. Rafique M, Sadaf I, Rafique MS, Tahir MB (2017) A review on green synthesis of silver nanoparticles and their applications. Artificial Cells, Nanomedicine Biotechnol 45:1272–1291. https://doi.org/10.1080/21691401.2016.1241792
30. Rai MK, Deshmukh SD, Ingle AP, Gade AK (2012) Silver nanoparticles: The powerful nanoweapon against multidrug-resistant bacteria. J Appl Microbiol 112:841–852. https://doi.org/10.1111/j.1365-2672.2012.05253.x
31. Rashid MH, Mandal TK (2007) Synthesis and catalytic application of nanostructured silver dendrites. J Phys Chem C 111:16750–16760. https://doi.org/10.1021/jp074963x
32. Ritthichai T, Pimpan V (2017) Ammonia sensing of silver nanoparticles synthesized using tannic acid combined with UV radiation: Effect of UV exposure time. J King Saud Univ - Sci 1:1–8. https://doi.org/10.1016/j.jksus.2017.10.003
33. Shen W, Zhang X, Huang Q, et al (2014) Preparation of solid silver nanoparticles for inkjet printed flexible electronics with high conductivity. Nanoscale 6:1622–1628. https://doi.org/10.1039/C3NR05479A
34. Shin KS, Cho YK, Choi JY, Kim K (2012) Facile synthesis of silver-deposited silanized magnetite nanoparticles and their application for catalytic reduction of nitrophenols. Appl Catal A Gen 413–414:170–175. https://doi.org/10.1016/j.apcata.2011.11.006
35. Shon YS, Cutler E (2004) Aqueous synthesis of alkanethiolate-protected Ag nanoparticles using bunte salts. Langmuir 20:6626–6630. https://doi.org/10.1021/la049417z
36. Siddiqui MN, Redhwi HH, Achilias DS, et al (2018) Green synthesis of silver nanoparticles and study of their antimicrobial properties. J Polym Environ 26:423–433. https://doi.org/10.1007/s10924-017-0962-0
37. Singh P, Kim YJ, Wang C, et al (2016) The development of a green approach for the biosynthesis of silver and gold nanoparticles by using Panax ginseng root extract, and their biological applications. Artificial Cells, Nanomedicine Biotechnol 44:1150–1157. https://doi.org/10.3109/21691401.2015.1011809
38. Sondi I, Goia DV., Matijević E (2003) Preparation of highly concentrated stable dispersions of uniform silver nanoparticles. J Colloid Interface Sci 260:75–81. https://doi.org/10.1016/S0021-9797(02)00205-9
39. Sylvia DH, Rajmuhon SN, David Singh T (2016) A benign approach for synthesis of silver nanoparticles and their application in treatment of organic pollutant. Arab J Sci Eng 41:2249–2256.

https://doi.org/10.1007/s13369-015-2007-0

40. Ali A, V. Baheti, J. Militky, Z. Khan, S.Q.Z. Gilani, " Comparative Performance of Copper and Silver Coated Stretchable Fabrics, " Journal of fiber and polymers. Vol 19, pp 607 , 2018
41. Tang S, Vongehr S, Meng X (2010) Carbon spheres with Ccntrollable silver nanoparticle doping. J Phys Chem C 114:977–982
42. Toisawa K, Hayashi Y, Takizawa H (2010) Synthesis of highly concentrated Ag nanoparticles in a heterogeneous solid-liquid system under ultrasonic irradiation. Mater Trans 51:1764–1768. https://doi.org/10.2320/matertrans.mj201005
43. Tran QH, Nguyen VQ, Le AT (2013) Silver nanoparticles: Synthesis, properties, toxicology, applications and perspectives. Adv Nat Sci Nanosci Nanotechnol 4:1–20. https://doi.org/10.1088/2043-6262/4/3/033001
44. Wang X, Cao W, Xiang Q, et al (2017) Silver nanoparticle and lysozyme/tannic acid layer-by-layer assembly antimicrobial multilayer on magnetic nanoparticle by an eco-friendly route. Mater Sci Eng C 76:886–896. https://doi.org/10.1016/j.msec.2017.03.192
45. Yang J, Yin H, Jia J, Wei Y (2011) Facile synthesis of high-concentration, stable aqueous dispersions of uniform silver nanoparticles using aniline as a reductant. Langmuir 27:5047–5053. https://doi.org/10.1021/la200013z
46. Zeng T, Zhang X, Guo Y, et al (2014) Enhanced catalytic application of Au@polyphenol-metal nanocomposites synthesized by a facile and green method. J Mater Chem A 2:14807–14811. https://doi.org/10.1039/C4TA02831G
47. Zhang W, Sun Y, Zhang L (2015) In situ synthesis of monodisperse silver nanoparticles on sulfhydryl-functionalized poly(glycidyl methacrylate) microspheres for catalytic reduction of 4-nitrophenol. Ind Eng Chem Res 54:6480–6488. https://doi.org/10.1021/acs.iecr.5b01010
48. Zheng Z, Huang Q, Guan H, Liu S (2015) In situ synthesis of silver nanoparticles dispersed or wrapped by a Cordyceps sinensis exopolysaccharide in water and their catalytic activity. RSC Adv 5:69790–69799. https://doi.org/10.1039/C5RA09452F